Biometals (2010) 23:1085–1095
DOI 10.1007/s10534-010-9354-9

Apolipoprotein E ablation decreases synaptic vesicular zinc in the brain

Joo-Yong Lee · Eunsil Cho · Tae-Youn Kim · Dong-Kyu Kim · Richard D. Palmiter · Irene Volitakis · Jong S. Kim · Ashley I. Bush · Jae-Young Koh

Received: 22 April 2010 / Accepted: 1 June 2010 / Published online: 17 June 2010

Abstract Both apolipoprotein E (apoE) and zinc are involved in amyloid β (Aβ) aggregation and deposition, in the hallmark neuropathology of Alzheimer's disease (AD). Recent studies have suggested that interaction of apoE with metal ions may accelerate amyloidogenesis in the brain. Here we examined the impact of apoE deficiency on the histochemically reactive zinc pool in the brains of apoE knockout mice. While there was no change in total contents of metals (zinc, copper, and iron), the level of histochemically reactive zinc (principally synaptic zinc) was significantly reduced in the apoE-deficient brain compared to wild-type. This reduction was accompanied by reduced expressions of the presynaptic zinc transporter, ZnT3, as well as of the δ-subunit of the adaptor protein complex-3 (AP3δ), which is responsible for post-translational stability and activity of ZnT3. In addition, the level of histochemically reactive zinc was also decreased in the cerebrovascular micro-vessels of apoE-deficient mice, the site of cerebral amyloid angiopathy in AD. These results suggest that apoE may affect the cerebral free zinc pool that contributes to AD pathology.

Keywords Alzheimer's disease · Amyloid β · Metal · Zinc transporters

J.-Y. Lee · E. Cho · T.-Y. Kim · D.-K. Kim · J.-Y. Koh
Asan Institute for Life Sciences, Asan Medical Center, Seoul 138-736, Republic of Korea

J.-Y. Lee · J. S. Kim · J.-Y. Koh
Department of Neurology, University of Ulsan College of Medicine, Seoul 138-736, Republic of Korea

T.-Y. Kim · D.-K. Kim · J.-Y. Koh (✉)
Neural Injury Research Laboratory, University of Ulsan College of Medicine, Seoul 138-736, Republic of Korea
e-mail: jkko@amc.seoul.kr

I. Volitakis · A. I. Bush (✉)
The Oxidation Disorders Laboratory, The Mental Health Research Institute, 155 Oak St., Parkville, VIC 3052, Australia
e-mail: a.bush@mhri.edu.au

I. Volitakis · A. I. Bush
Department of Pathology, The University of Melbourne, Melbourne, VIC 3010, Australia

R. D. Palmiter
Department of Biochemistry, Howard Hughes Medical Institute, University of Washington, Seattle, WA 98195, USA

Introduction

The brain is the second most abundant tissue for apolipoprotein (apoE) after liver. In the normal brain, apoE is generated primarily by astrocytes and microglia, while neurons express little (Boyles et al. 1985; Nakai et al. 1996). In humans, apoE is found as three isoforms (apoE2, apoE3, and apoE4) that differ by single amino acid substitutions. ApoE3 is the most common isoform, while apoE4 expression is the most

detrimental to brain health for several disease states (Zhao et al. 1993; Bales et al. 2009). The genetic dose of apoE4 is the strongest risk factor for the incidence of sporadic Alzheimer's disease (AD) (Saunders et al. 1993).

The oligomerization and deposition of amyloid-β (Aβ) in the brain is centrally involved in AD (Bu 2009) but the cause for the age-dependent aggregation of this ubiquitously-expressed peptide remains unknown. Mounting evidence indicates that apoE is involved in AD pathogenesis. ApoE that binds to Aβ with high affinity (Strittmatter et al. 1993; Sanan et al. 1994; Näslund et al. 1995) is enriched in parenchymal or cerebrovascular amyloid deposits and in neurofibrillary tangles in the brains of AD patients and of amyloid-β protein precursor (APP) transgenic mice that serve as a model for AD (Namba et al. 1991; Wisniewski and Frangione 1992; Strittmatter et al. 1993; Benzing and Mufson 1995). Genetic ablation of apoE leads to a reduction in Aβ deposition, despite unchanged Aβ generation, in APP-transgenic mice (Bales et al. 1997, 1999; Holtzman et al. 2000). The interactions of apoE with APP/Aβ via its receptors modulate Aβ processing, clearance and degradation in the brain (Zhao et al. 1993; Koistinaho et al. 2004; Offe et al. 2006; Deane et al. 2008; Jiang et al. 2008).

Extracellular zinc (Zn^{2+}) concentrations may be a critical factor for AD pathogenesis. Zn^{2+} is markedly enriched in amyloid plaques (Lovell et al. 1998; Lee et al. 1999; Suh et al. 2000; Miller et al. 2006), consistent with the Zn^{2+} inducing Aβ aggregation (Bush et al. 1994; Miura et al. 2000; Yang et al. 2000). Meanwhile, Zn^{2+}-chelators resolubilize Aβ aggregates (Cherny et al. 1999) and attenuate amyloid load in Tg2576 APP-transgenic mice (Cherny et al. 2001; Lee et al. 2004a, b; Adlard et al. 2008). Deposition of amyloid plaques in AD brain occurs along with the distribution of synaptic zinc (Stoltenberg et al. 2007; Deshpande et al. 2009), which is the free zinc pool sequestered within synaptic vesicles and is released upon synaptic activity (Palmiter et al. 1996; Frederickson et al. 2005). Genetic ablation of zinc transporter-3 (*Slc30a3*/*ZnT3*), which concentrates Zn^{2+} into synaptic vesicles, decreases total brain zinc levels by $\approx$20%, and markedly attenuates the deposition of amyloid plaques and cerebral amyloid angiopathy (CAA) in Tg2576 mice (Lee et al. 2002; Friedlich et al. 2004). Furthermore, a growing body of evidence has supported the chemical interaction between Aβ and Zn^{2+}. The three histidine residues (H6, H13, and H14) within the hydrophilic N-terminal of Aβ mediate the affinity for Zn^{2+} (Bush et al. 1993; Atwood et al. 1998; Syme and Viles 2006; Danielsson et al. 2007) with a stoichiometry of Zn^{2+}:Aβ of 1–3:1 (Clements et al. 1996; Atwood et al. 2000). Other carboxylate side chain amino acids, aspartic acid (D1) and glutamic acid (E11) also can bind Zn^{2+} (Mekmouche et al. 2005; Syme and Viles 2006; Zirah et al. 2006; Danielsson et al. 2007). The Zn^{2+}-bridges between the histidine residues within different Aβ molecules leads to amorphous Aβ aggregates (Miura et al. 2000; Syme and Viles 2006), which is relatively soluble and stable (Kozin et al. 2001). These findings implicate free zinc, in particular synaptic zinc, in amyloid pathogenesis.

Therefore, most amyloid plaques contain both Zn^{2+} and apoE (Fig. 1), consistent with the amphipathic chemical structure of Aβ that supports metal ion as well as lipid binding. There are several metal-binding moieties at the hydrophilic N-terminal of Aβ (Bush et al. 1993; Atwood et al. 1998), while the C-terminus binds lipoproteins such as apoE by hydrophobicity (Kontush 2005). The various apoE isoforms have interactions with Zn^{2+} that are in concordance with the predicted loss of affinity that is a consequence of the Arg–Cys substitutions (Miyata and Smith 1996; Moir et al. 1999). Cys being a strong ligand for Zn^{2+}, and Arg not being a ligand for Zn^{2+}, the affinity for Zn^{2+} is predicted to be greatest for apoE2 and weakest for apoE4. This likelihood is supported by the effects of apoE isoforms in protecting cells from Zn^{2+}-induced neurotoxicity (Miyata and Smith 1996) and by protecting Aβ from zinc-induced precipitation (Moir et al. 1999). ApoE2 preferentially binds Zn^{2+} so preventing Aβ-oligomerization and aggregation (Moir et al. 1999). In contrast, because apoE4 has the lowest affinity of the isoforms for metal ions, Aβ is more readily able to interact with the surrounding metals to be oligomerized and aggregate. However, although zinc is significantly elevated in the serum of AD patients who carry the genetic allele (ε4) for apoE4 (González et al. 1999), to date the impact of apoE expression on brain Zn^{2+} biochemistry is unknown.

The aim of this study is to test whether apoE expression impacts upon the histochemically reactive zinc pool in the brain, a fraction of total tissue zinc

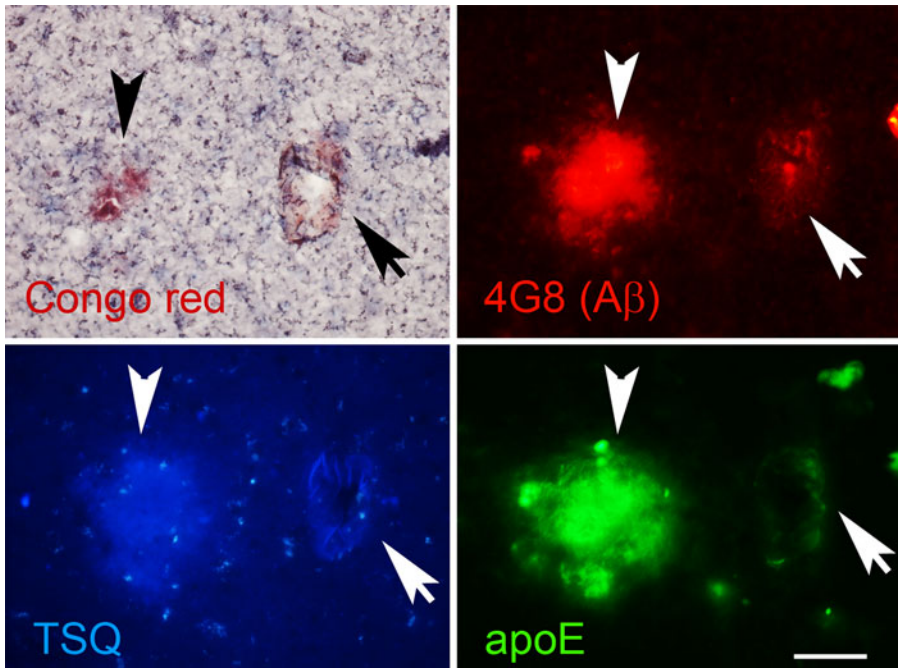

Fig. 1 Co-localization of apoE and Zn^{2+} in amyloid pathology. Histofluorescently reactive zinc and apoE were detected in parenchymal (*arrowheads*) and cerebrovascular (*arrows*) amyloid deposits. Brain tissue of Tg2576 APP-transgenic mouse at the age of 21 months was stained with TSQ (blue fluorescence) and doubly immuno-stained with anti-Aβ (4G8) (red fluorescence) and anti-apoE (green fluorescence) antibodies, and then photographed at intervals between the stains. The same section was finally histochemically stained with Congo red (dark red). Magnification ×400; scale bar, 50 μm

that is implicated in amyloid precipitation. In the brains of mice lacking the gene for apoE, histofluorescent synaptic zinc, representative of intracerebral free zinc pool, was significantly decreased in conjunction with decreased expression of ZnT3. In addition, levels of histochemically reactive zinc in the cerebrovasculature were diminished in apoE-deficient mice.

Materials and methods

Animal studies

Studies were performed in accordance with the Guidelines of the Asan Institute for Life Sciences for Experimental Animal Care and Use.

Mice homozygous for the *Apoe*^{tm1Unc} mutation (Strain name: B6.129P2-*Apoe*^{tm1Unc}/J) (The Jackson Laboratory; Bar Harbor, ME) were crossed with C57BL/6 mice and the resulting heterozygous mice were interbred to produce apoE wild-type (*apoE*$^{+/+}$) and apoE-deficient (*apoE*$^{-/-}$) mice in Asan Institute for Life Sciences, Asan Medical Center (Seoul, Korea).

Tissue preparations

Brains were removed and divided into two hemispheres. The right hemispheres were snap-frozen in liquid nitrogen and the left hemispheres were processed for further metal or protein assays.

For histological evaluation, five coronal sections (12 μm thick) of the right hemisphere, which were taken every 12 μm from bregma-1.3 mm using a cryostat (HM550; Microm International GmbH, Walldorf, Germany), were mounted on gelatin-coated slide glasses.

Measurement of total contents of metals by inductively coupled plasma mass spectroscopy (ICP-MS)

Tissues (brain, liver, heart, and blood plasma) were weighed, lyophilized, and then transported to The

Mental Health Research Institute of Victoria (Victoria, Australia), where the metal contents were analyzed by ICP-MS. The tissues were digested in ultrapure HNO_3 (Aristar, BDH, Poole, UK) by heating, and then dried by evaporation. After an appropriate dilution with 1% HNO_3, three replicates per tissue sample were analyzed using an Ultramass 700 spectrophotometer (Varian, Victoria, Australia) that was calibrated using 1% HNO_3 containing Cu, Fe and Zn at 5, 10, 50, and 100 ppb, with 89Y as the internal standard for all isotopes of Cu, Fe and Zn.

Zinc specific fluorescent staining and measurement of the free zinc

We stained brain sections with a zinc-specific fluorescent dye, *N*-(6-methoxy-8-quinolyl)-*p*-toluenesulfonamide (TSQ, 4.5 μM in 140 mM sodium barbital and 140 mM sodium acetate buffer, pH 10.0; Molecular Probes, Eugene, OR) for 90 s (Lee et al. 2002, 2004a, b). After a dipping in normal saline (0.9% NaCl solution, pH 7.2), the fluorescent sections were examined and photographed under a fluorescence microscope (UV-2A filter: dichroic, 400 nm; excitation, 330–380 nm; barrier, 420 nm) (Eclipse 80i; Nikon, Tokyo, Japan) with a digital camera (DS-Fi1/DS-U2; Nikon) and the manufacturer's imaging capture program (NIS-Elements F; Nikon).

We quantified the level of TSQ-fluorescence in the defined regions of interest (ROIs) in the hippocampal mossy fiber region (asterisked area in Fig. 2), the area which contains the high concentration of synaptic zinc, and in longitudinally dissected blood vessels with diameter of 30–80 μm (arrows in Fig. 4). Fluorescence intensity was determined with a computer-assisted image analysis program (Image-Pro; Media Cybernetics, Silver Spring, MD). After subtraction of background fluorescence (taken at an area outside of tissue section), the level of free zinc was expressed as percent TSQ-fluorescence intensity relative to that in normal wild-type mice sections (defined as a value of 100%).

Fluorescent immunohistochemistry

For immunohistochemical staining, we used the following primary antibodies; mouse anti-Aβ antibody (4G8, dilution 1:800; Signet, Dedham, MA), rabbit anti-ZnT3 antibody (1:50) (Cole et al. 1999), mouse anti-synaptophysin antibody (SYP, 1:100; Sigma, St. Louis, CA) and mouse anti-smooth muscle actin antibody (1:200; Chemicon, Temecula, CA).

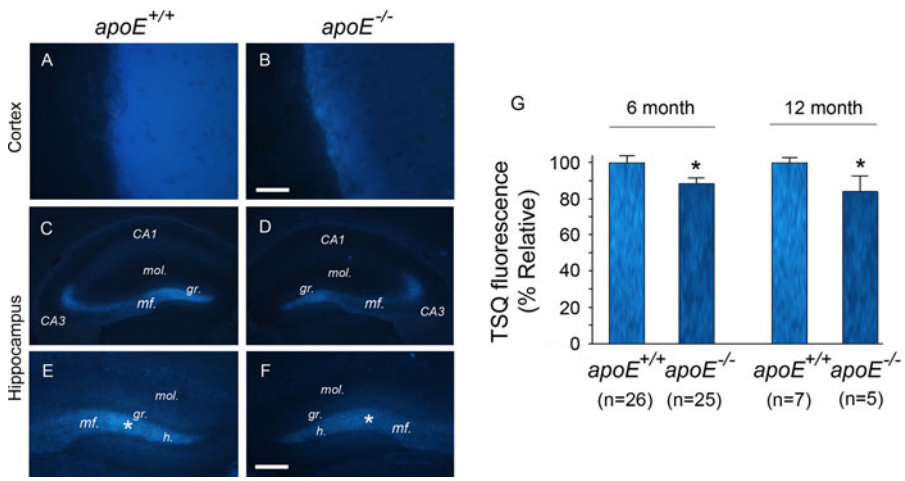

Fig. 2 apoE expression influences histochemically reactive zinc in the brain. Brain sections from $apoE^{+/+}$ or $apoE^{-/-}$ mice were stained with TSQ at the age of 6 or 12 months. **a**–**f** TSQ-fluorescence was attenuated throughout the whole brain containing cortex (**a** and **b**) or hippocampus (**c**–**f**) in $apoE^{-/-}$ mice (**b**, **d**, and **f**) compared to $apoE^{+/+}$ mice (**a**, **c**, and **e**) at the age of 12 months. *mol.* dentate molecular layer, *gr.* dentate granular layer, *h.* dentate hilus. *mf.* mossy fiber. Scale bars, 200 μm (**a**–**d**) and 50 μm (**e** and **f**). **g** Quantification of synaptic zinc in the mouse brain at the age of 6 or 12 months. Bars denote the relative intensity of TSQ-fluorescence measured in the mossy fiber regions (*asterisked areas* in **e** and **f**) in both hippocampi of five brain sections, which were taken every 100 μm from bregma +4.3 mm (mean ± SEM). *Asterisk* denotes significant difference between two genotypes of mice (* $P < 0.05$)

Frozen brain sections were fixed with 4% (w/v) paraformaldehyde [in phosphate buffered saline (PBS), pH 7.4]. After incubation in blocking buffer (3% normal donkey serum and 0.3% Triton X-100 in PBS), the sections were immunologically reacted with the primary antibody, and then with Alexa Fluor 488- or 555-conjugated secondary antibody (1:1000; Invitrogen, Carlsbad, CA). The stained tissues were examined and photographed under a fluorescence microscope (Eclipse 80i).

Immunoblot analysis

The brain tissues were homogenized in PRO-PREP™ protein extraction solution (iNtRON, Seoul, Korea). After sonicating and boiling in sample buffer (62.5 mM Tris, pH 6.8, 2% SDS, 10% glycerol, 0.01% bromophenol blue, 5% mercaptoethanol, 50 mM dithiothreitol), proteins were separated by sodium dodecyl sulfate-polyacrylamide gel electrophoresis (SDS-PAGE) and transferred onto polyvinylidene difluoride membranes (Immobilon-PSQ Transfer Membrane; Millipore). The membrane blots were blocked with 5% skim milk and 1% bovine serum albumin (BSA; Amresco, Solon, OH) in TBST buffer (pH 7.4; 20 mM Tris–Cl, 150 mM NaCl, 0.01% Tween 20) and then reacted with primary antibody [goat anti-apoE (dilution, 1:1000; Santa Cruz, Santa Cruz, CA), goat anti-ZnT1 (1:1000; Santa Cruz), rabbit anti-ZnT3 (1:2500), mouse anti-synaptophysin (SYP, 1:1000; Sigma), goat anti-AP3δ (1:2500; Lifespan, Seattle, WA), or mouse anti-β-actin (1:4000; Sigma) antibody]. After washing with TBST, blots were incubated with horseradish peroxidase-conjugated secondary anti-rabbit, -goat, or -mouse antibody. Finally, proteins were visualized using enhanced chemiluminescence reagents (Immobilon Western Chemiluminescent HRP Substrate; Millipore, Billerica, MA) under a chemiluminescence imaging system (KODAK Image Station 4000MM Pro.; Carestream Health, Rochester, NY).

Statistical analysis

All values are presented as mean ± standard error of the mean. Differences between apoE-wild-type and -deficient mice were determined by the unpaired *t*-test with a two-tailed *P* value. A *P* value less than 0.05 was considered significant.

Results

Metal content in the apoE-wild-type and -deficient mice

Metal analysis for iron (Fe), zinc (Zn) and copper (Cu) were performed in four tissues (brain, liver, heart, and blood plasma) from apoE-wild-type and apoE-deficient mice (Table 1) at the age of 6 months. Total levels of metals vary with different tissues, but the abundance was in the order of Fe > Zn > Cu for each tissue. However, there was no significant difference in the level of iron, zinc or copper in all tissues between apoE-wild-type and -deficient mice.

Decreased level of cerebral free zinc in the apoE-deficient mice

Since apoE binds transition metal ions (Miyata and Smith 1996; Moir et al. 1999), we hypothesized that the ablation of apoE might alter the fraction of free zinc in the brain. To differentiate free Zn^{2+} from total zinc in the brain, we stained brain sections with TSQ, which is a well-characterized fluorophore for exchangeable Zn^{2+} (Lee et al. 2002). TSQ detected exchangeable Zn^{2+} in amyloid plaques, where it colocalized with apoE (Fig. 1). In comparison to wild-type tissue,

Table 1 Metal contents in various tissues of apoE-wild-type ($apoE^{+/+}$) and knock-out ($apoE^{-/-}$) mice at the age of 6 months (μg/g of wet tissue; $n = 25$, each)

Tissue	Metal	Genotype		*P* value[#]
		$apoE^{+/+}$	$apoE^{-/-}$	
Brain	Cu	3.81 ± 0.05[a]	3.72 ± 0.05	0.271
	Fe	17.12 ± 0.24	16.59 ± 0.25	0.124
	Zn	14.63 ± 0.18	14.73 ± 0.25	0.761
Liver	Cu	4.82 ± 0.18	4.62 ± 0.19	0.448
	Fe	84.45 ± 4.86	84.12 ± 5.31	0.958
	Zn	28.83 ± 0.30	27.84 ± 0.39	0.051
Heart	Cu	6.58 ± 0.10	6.64 ± 0.08	0.642
	Fe	81.34 ± 1.57	85.55 ± 1.96	0.100
	Zn	16.51 ± 0.24	16.64 ± 0.26	0.725
Plasma	Cu	6.35 ± 0.23	6.83 ± 0.26	0.166
	Fe	38.85 ± 2.03	38.74 ± 3.15	0.977
	Zn	13.32 ± 0.57	13.01 ± 0.58	0.696

[#] Differences between two genotypes of mice were determined by the unpaired t-test with two tailed *P* value

[a] Mean ± SEM

TSQ-fluorescence was significantly diminished in apoE-deficient cortex and hippocampus (Fig. 2a–d). This is consistent with the expression of apoE increasing the histochemically reactive zinc pool in the brain.

Synaptic Zn^{2+} constitutes 20–30% of total brain zinc and is the most abundant pool of free zinc in this tissue, especially in the mossy fiber region (Cole et al. 1999; Lee et al. 2002). Therefore, we measured TSQ-fluorescence in the defined ROI in the hippocampal mossy fiber region (*mf* in Fig. 2). At the age of 6 months, the level of synaptic Zn^{2+} is decreased by 11.5% in apoE-deficient mice compared to wild-type mice ($88.5 \pm 3.4\%$ vs. $100.0 \pm 3.8\%$, $P < 0.05$) (Fig. 2e). At the age of 12 months, the contribution of apoE to synaptic Zn^{2+} is significantly greater (15.2%; $84.8 \pm 8.2\%$ vs. $100.0 \pm 2.5\%$, $P < 0.05$).

Altered expression of ZnT3 protein in apoE-deficient mice

We next examined whether the decrease in histochemically reactive zinc in apoE-deficient brain could be due to altered the levels of ZnT1 or ZnT3, which are responsible for Zn^{2+} efflux from cells or sequestration of Zn^{2+} in synaptic vesicles, respectively (Palmiter and Huang 2004), and synaptophysin, a marker of presynaptic terminals.

Immunohistofluorescent staining revealed that the ablation of apoE led to the reduced expression of ZnT3 protein, in parallel with the reduction of synaptic zinc. Anti-ZnT3 immunoreactivity was significantly attenuated throughout the whole brain of the apoE-knockout mice compared to wild-type mice (Fig. 3a–d). Moreover, western blot assay detected a $\approx$21% decrease in ZnT3 expression (Fig. 3g, h). In contrast, there was no difference in expression of ZnT1 between two genotypes of mice (Fig. 3g). Because ZnT3 is present in the membrane of synaptic vesicles, degeneration of nerve terminals can potentially result in losses of ZnT3 and synaptic zinc. Despite the an earlier report that apoE deficiency resulted in the loss of synaptophysin-immunoreactive nerve terminals in the mouse brain at this age (Masliah et al. 1995), the immunoreactive expression

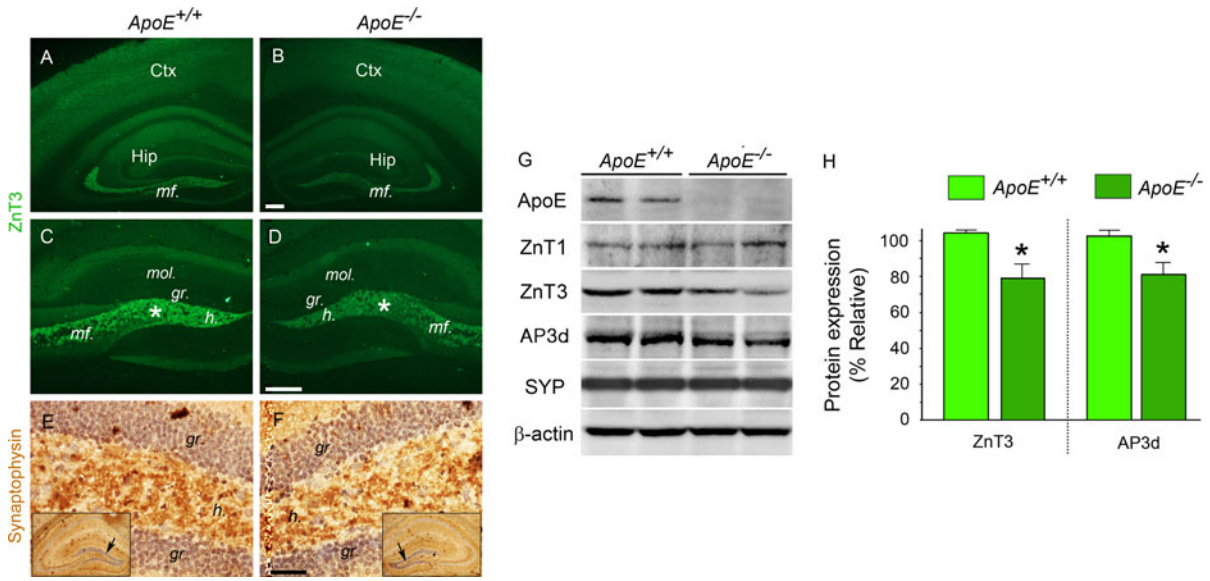

Fig. 3 Expressions of ZnT1, ZnT3, AP3δ, and synaptophysin in the brains of $apoE^{+/+}$ or $apoE^{-/-}$ mice at the age of 12 months. **a**, **b** Brain sections containing cortex (Ctx) and hippocampus (Hip) were immunofluorescently stained with anti-ZnT3 antibody (magnification, 40×). **c**, **d** High power magnification (100×) of dentate gyrus in hippocampus regions that were immunostained with anti-ZnT3 antibody. *mf.* mossy fiber, *mol.* dentate molecular layer, *gr.* dentate granular layer, *h.* dentate hilus. **e**, **f** High power magnification (400×) of synaptophysin-immunostained hippocampal dentate hilar regions (*arrows* in *insets*). Scale bars, 250, 50, and 25 μm. **g** Representative immunoblots of brain lysates for apoE, ZnT1, ZnT3, AP3δ, synaptophysin (SYP) or β-actin. **h** Densitometric quantifications of ZnT3 and AP3δ protein expression. The optical density of ZnT3 or AP3δ immunoreactivity ($n = 4$ samples) was normalized to that of β-actin as an internal control, and then values relative to wild-type mice were depicted as bars (mean ± SEM). *Asterisks* represent significant differences between two genotypes of mice ($P < 0.05$, $n = 4$ animals for each genotype)

levels of synaptophysin were unchanged in our apoE-knockout mice (Fig. 3e–g). These results suggest that the reduced level of histochemically reactive zinc in the brains of apoE-knockout mice is responsive to the down-regulated expression of ZnT3, but not due to synaptic degeneration.

The δ-subunit of adaptor protein complex (AP3δ) is responsible for the post-translational stability and activity of ZnT3 in synaptic vesicles (Salazar et al. 2004). AP3δ-deficient *mocha* mice are devoid of both ZnT3 and synaptic zinc in their brains (Kantheti et al. 1998). Therefore, we determined the expression level of AP3δ in the apoE-knockout mice (Fig. 3g, h). Western blot assay indicated a significantly reduced level of AP3δ (-18.3%, $P < 0.05$) in apoE-deficient mice compared to wild-type mice. Therefore, apoE expression may modulate the levels of ZnT3 and synaptic zinc via alteration of AP3δ activity.

Histochemically reactive free zinc pool in the cerebrovasculature

Apart from plaques, we found zinc-specific TSQ-fluorescence and apoE-immunoreactivity to be colocalized also in the cerebrovascular amyloid pathology of aged Tg2576 mice (Fig. 1). As Zn^{2+} (Friedlich et al. 2004) as well as apoE (Fryer et al. 2003) have both been implicated in the formation of CAA, we examined whether apoE ablation also affects histochemically reactive free zinc levels in cerebral blood vessel walls.

TSQ-staining confirmed the presence of intense zinc-specific fluorescence in cerebral blood vessels of wild-type mice and the intensity of TSQ-fluorescence was significantly attenuated in apoE-null mice by ≈ 8 ($92.0 \pm 2.1\%$ vs. $100.0 \pm 2.0\%$, $P < 0.01$) and 11% ($89.1 \pm 3.6\%$ vs. $100.0 \pm 2.3\%$, $P < 0.05$), at the ages of 6 and 12 months, respectively (Fig. 4), similar to the decrease in synaptic zinc associated with apoE ablation (Fig. 2). In contrast, ZnT3 immunoreactivity was not detected in cerebral blood vessels (Fig. 5), as described previously (Friedlich et al. 2004). We previously demonstrated that the cerebrovascular zinc pool reflects the exchange of Zn^{2+} released from ZnT3-containing synaptic boutons with the cerebrovascular wall (Friedlich et al. 2004). Thus, apoE may affect the deposition of free zinc in the cerebrovascular wall by modulating the expression of ZnT3 in the parenchymal synaptic terminals.

Discussion

This study demonstrates that apoE expression indirectly elevates the free zinc pool in the brain. While we initially considered that the free zinc level might be increased in apoE-deficient mice because of the loss of metal-chelating apoE, the levels of histochemically reactive free zinc actually diminished throughout the cortex and hippocampus (Fig. 2). The loss of histochemically reactive zinc was associated with decreased expression of ZnT3 (Fig. 3). Therefore, apoE appears to elevate the intravesicular levels of free zinc by promoting the expression of ZnT3 protein. Notably, total zinc remained unchanged in all apoE-null tissues tested, including brain (Table 1). Since the vesicular Zn^{2+} pool represents about 20–30% of total cerebral zinc (Cole et al. 1999; Lee et al. 2002), and since ablation of apoE is associated with an 11.5% decrease in the vesicular Zn^{2+} pool (Fig. 4e), the anticipated decrease in total cerebral zinc in the apoE-null tissue was ≈ 2.3–3.5% at the age of 6 months. Based upon the variance in the zinc levels in our samples (Table 1), our study was more than adequately powered to detect such a difference. Therefore, it is possible that apoE plays a role in the presentation of free zinc to synaptic vesicles, and in the absence of apoE, Zn^{2+} collects in a non histochemically-reactive form in the neuronal soma or elsewhere, so that there is no net loss of total tissue zinc.

Upon synaptic activity, Zn^{2+} is released into synaptic cleft, where most of it enters post-synaptic neurons to modulate synaptic transmission or is reabsorbed into presynaptic neurons and recycled (Frederickson et al. 2005), but some drains into brain vessels via the interstitial and perivascular basement membranes (Friedlich et al. 2004; Carare et al. 2008). In Fig. 5 and in our previous report (Friedlich et al. 2004), we found no ZnT3 in the cerebrovasculature, and that ZnT3 ablation alone lowers histochemical zinc in the cerebrovascular wall (Friedlich et al. 2004). These findings suggest that the histofluorescent zinc in this tissue is not in vesicles, and that its drop must be caused by ZnT3 acting at a distance; probably through the release of zinc that migrates in the interstitial spaces to the cerebrovasculature. Thus, neuronal zinc in the brain parenchyma may communicate with the cerebrovasculature through this route, which is likely how Zn^{2+} accumulates within CAA in AD and in APP-transgenic mice (Suh et al. 2000;

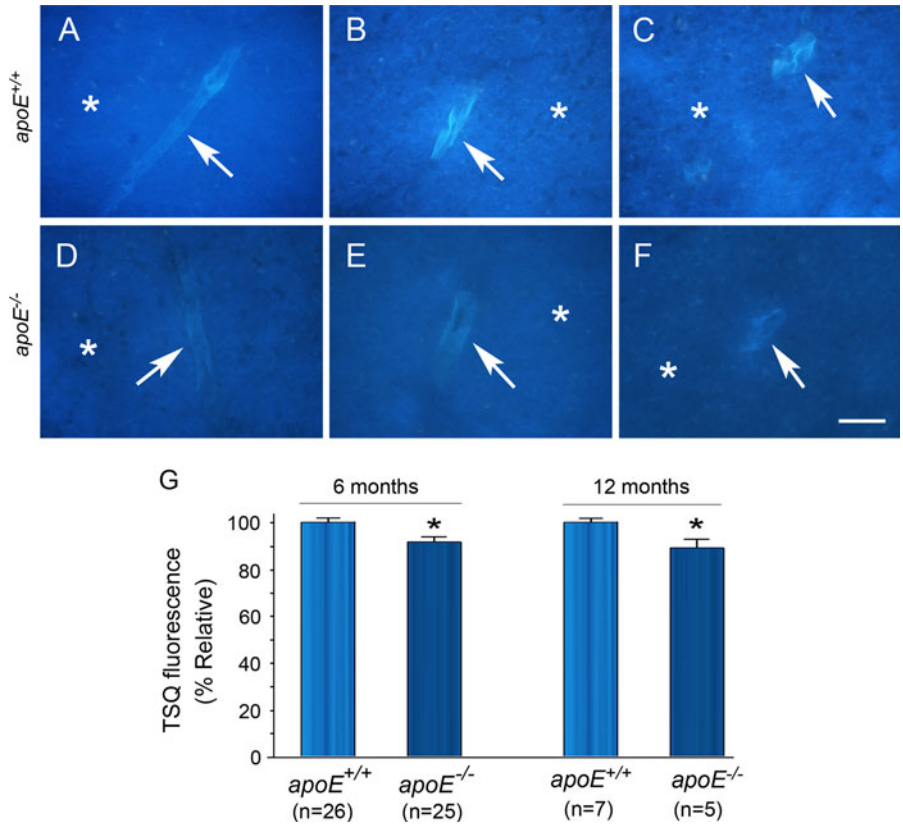

Fig. 4 Histochemically reactive zinc in cerebral blood vessel walls. **a–h** Longitudinally dissected blood vessels (*arrows*) were fluorescently stained with TSQ in the identical brain areas of apoE wild-type ($apoE^{+/+}$; **a–c**) and knock-out ($apoE^{-/-}$; **d–f**) mice at the age of 12 months. The intensity of TSQ fluorescence in vessel walls (*arrows*) as well as the parenchyma (*asterisks*) was attenuated in $apoE^{-/-}$ mice as compared to $apoE^{+/+}$ mice. Scale bar, 50 μm. **g** Comparison of histofluorescent zinc in the cerebral blood vessels at the age of 6 or 12 months. *Bars* denote the relative intensity of TSQ-fluorescence measured in longitudinally dissected blood vessels (mean ± SEM, $n = 100$ vessels per animal). *Asterisks* denote significant difference between two genotypes of mice (* $P < 0.01$ and ** $P < 0.05$)

Friedlich et al. 2004). In the current study we find that apoE ablation causes about 10% decrease in histochemical zinc in the cerebrovasculature (Fig. 4), in parallel with a 20% decrease in ZnT3 expression in the brain parenchyma (Fig. 3). The most likely explanation for the decrease in histochemical zinc in the cerebrovasculature of the $apoE^{-/-}$ mice is therefore the drop in ZnT3 expression, although other explanations, such as loss of Zn^{2+} coordination by apoE present in the cerebrovasculature cannot be excluded. Our previous studies have shown that ZnT3 expression contributes 20% to the histochemically reactive free zinc pool of the cerebrovascular wall (Friedlich et al. 2004). Therefore, apoE accounts for ≈40% of the cerebrovascular wall Zn^{2+} that is associated with ZnT3 expression.

Genetic ablation of either ZnT3 (Lee et al. 2002; Friedlich et al. 2004) or apoE (Fryer et al. 2003) both cause marked (≈80%) decreases in amyloid pathology in APP transgenic mice. Could apoE ablation rescue amyloid pathology in transgenic mice by lowering "amyloidogenic" Zn^{2+} originating from ZnT3-mediated release? Our data indicate that apoE expression can account for as much as 40% of potentially amyloidogenic Zn^{2+} in the cerebrovasculature (Fig. 4), but only 11.5–15.2% of synaptic amyloidogenic Zn^{2+} (Fig. 2). Therefore, the most likely hypothesis is that synaptic Zn^{2+} could mediate some but not all of the amyloidogenic effects of apoE. Since ablation of either apoE or ZnT3 abolishes amyloid pathology, it appears that each factor is necessary but not sufficient to cause the

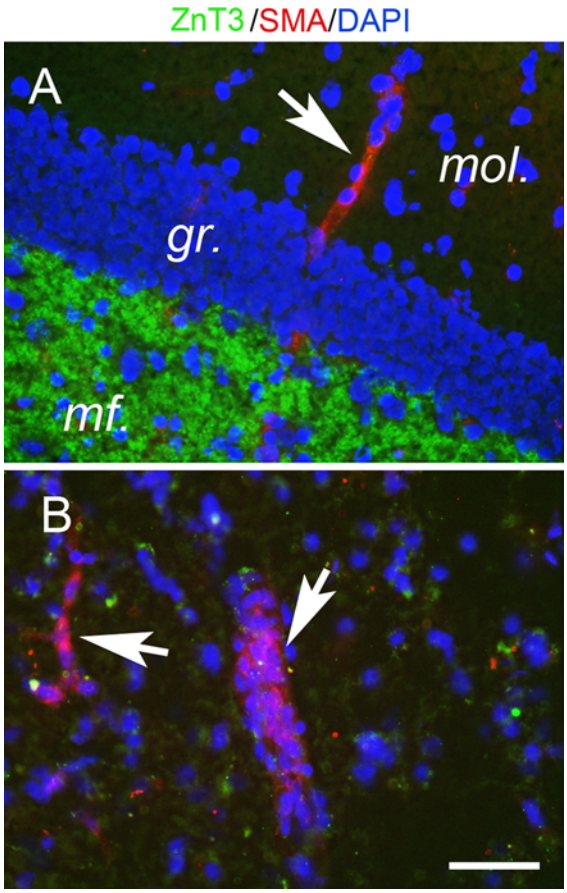

Fig. 5 Absence of ZnT3 in the cerebrovascular walls. Although ZnT3 immunoreactivity (green fluorescence) is present in the hippocampal mossy fiber region (*mf.* in **a**) of apoE wild-type mice, the blood vessels with the immunoreactivity for α-smooth muscle actin (SMA) (*arrows*; red fluorescence) lack ZnT3 throughout the brain, including hippocampus (**a**) or cortex (**b**). DAPI (4′,6-diamidino-2-phenylindole; blue fluorescence) stained nuclei in the neurons. *mf.* mossy fiber, *gr.* dentate granule layer, *mol.* dentate molecular layer. Scale bar, 50 μm

pathology. Our current data are consistent with an interplay between subpopulations of apoE and synaptic Zn^{2+} whose interaction causes pathology.

Although the fraction of histochemical zinc in the mossy fibers mediated by apoE seems modest (≈15%), we argue that the additive effect of such a decrease over time is sufficient to contribute to Aβ deposition. Since abnormal zinc homeostasis persists for many years in the evolution of AD pathology, even a small change of exchangeable zinc levels would influence the aggregation of Aβ. Moreover, the difference is significantly exaggerated by age (from 11% at 6 months to 15% at 12 months).

There is no obvious mechanistic explanation for how apoE might modulate ZnT3 expression in the brain. Because ZnT3 resides in the synaptic vesicle membrane of nerve terminals (Cole et al. 1999; Palmiter and Huang 2004; Frederickson et al. 2005), we needed to exclude synaptic degeneration as an explanation for ZnT3 and synaptic Zn^{2+} loss. We found no differences in synaptic integrity between our apoE-deficient and wild-type control mice, as determined by immunohistochemistry and western blot analysis for synaptophysin (Fig. 3). While these findings are at variance with those of Masliah et al. (1995), they are in agreement with the findings of Anderson et al. (1998) who also found no difference in synaptophysin and microtubule-associated protein 2 levels, markers for synaptic and dendritic densities respectively, between apoE knockout mice and wild-type controls. By contrast, in the brains of apoE-deficient mice, there was the significant reduction in the expression level of AP3δ (≈18.3%) (Fig. 3). AP3δ is critical to the post-translational stability and activity of ZnT3 in synaptic vesicles (Salazar et al. 2004). The *mocha* mice with the AP3δ-null mutation are devoid of both ZnT3 and synaptic zinc in their brains (Kantheti et al. 1998). We have previously reported that estrogen alters the ZnT3 and synaptic zinc levels in mouse brain, via changing AP3δ expression (Lee et al. 2004b). Therefore, the mechanism of apoE-mediated ZnT3 expression could be dependent on AP3 activity.

Since apoE isoforms have differential binding interactions with Zn^{2+} that are in concordance with their risk for AD, we hypothesize that the expression of the different apoE isoforms will increase the free zinc pools that we have described here in concordance with that risk (i.e. E4 > E3 > E2). Testing this in experimental systems will be challenging, since the pool of amyloidogenic extracellular Zn^{2+} is a minor fraction of total zinc in the brain, and the differential influence of the isoforms on this pool is likely to be subtle, in alignment with the many years that it takes for their expression to modulate amyloid pathology in humans.

Acknowledgements This study was supported by funds from the Korea Healthcare Technology R&D Project, Ministry for Health and Welfare, Republic of Korea (A080201 to JYL),

from Asan Institute for Life Sciences (2008-396 to JYL), from the Korea Research Foundation (NRL2009-0066335 and KPSEP2009-0081487 to JYK), and from the National Health and Medical Research Council of Australia, Australian Research Council and the Alzheimer's Association (to AIB).

References

Adlard PA, Cherny RA, Finkelstein DI et al (2008) Rapid restoration of cognition in Alzheimer's transgenic mice with 8-hydroxy quinoline analogs is associated with decreased interstitial Aβ. Neuron 59:43–55

Anderson R, Barnes JC, Bliss TV et al (1998) Behavioural, physiological and morphological analysis of a line of apolipoprotein E knockout mouse. Neuroscience 85: 93–110

Atwood CS, Moir RD, Huang X et al (1998) Dramatic aggregation of Alzheimer Aβ by Cu(II) is induced by conditions representing physiological acidosis. J Biol Chem 273:12817–12826

Atwood CS, Scarpa RC, Huang X, Moir RD et al (2000) Characterization of copper interactions with alzheimer amyloid beta peptides: identification of an attomolar-affinity copper binding site on Aβ1-42. J Neurochem 75: 1219–1233

Bales KR, Verina T, Dodel RC et al (1997) Lack of apolipoprotein E dramatically reduces amyloid β-peptide deposition. Nat Genet 17:263–264

Bales KR, Verina T, Cummins DJ et al (1999) Apolipoprotein E is essential for amyloid deposition in the APP(V717F) transgenic mouse model of Alzheimer's disease. Proc Natl Acad Sci USA 96:15233–15238

Bales KR, Liu F, Wu S et al (2009) Human APOE isoform-dependent effects on brain β-amyloid levels in PDAPP transgenic mice. J Neurosci 29:6771–6779

Benzing WC, Mufson EJ (1995) Apolipoprotein E immunoreactivity within neurofibrillary tangles: relationship to Tau and PHF in Alzheimer's disease. Exp Neurol 132:162–171

Boyles JK, Pitas RE, Wilson E, Mahley RW, Taylor JM (1985) Apolipoprotein E associated with astrocytic glia of the central nervous system and with nonmylinating glia of the peripheral nervous system. J Clin Invest 76:1501–1513

Bu G (2009) Apolipoprotein E and its receptors in Alzheimer's disease: pathways, pathogenesis and therapy. Nat Rev Neurosci 10:333–344

Bush AI, Multhaup G, Moir RD et al (1993) A novel zinc(II) binding site modulates the function of the βA4 amyloid protein precursor of Alzheimer's disease. J Biol Chem 268:16109–16112

Bush AI, Pettingell WH, Multhaup G et al (1994) Rapid induction of Alzheimer Aβ amyloid formation by zinc. Science 265:1464–1467

Carare RO, Bernardes-Silva M, Newman TA et al (2008) Solutes, but not cells, drain from the brain parenchyma along basement membranes of capillaries and arteries: significance for cerebral amyloid angiopathy and neuroimmunology. Neuropathol Appl Neurobiol 34:131–144

Cherny RA, Legg JT, McLean CA et al (1999) Aqueous dissolution of Alzheimer's disease Aβ amyloid deposits by biometal depletion. J Biol Chem 274:23223–23228

Cherny RA, Atwood CS, Xilinas ME et al (2001) Treatment with a copper-zinc chelator markedly and rapidly inhibits β-amyloid accumulation in Alzheimer's disease transgenic mice. Neuron 30:665–676

Clements A, Allsop D, Walsh DM, Williams CH (1996) Aggregation and metal-binding properties of mutant forms of the amyloid Aβ peptide of Alzheimer's disease. J Neurochem 66:740–747

Cole TB, Wenzel HJ, Kafer KE, Schwartzkroin PA, Palmiter RD (1999) Elimination of zinc from synaptic vesicles in the intact mouse brain by disruption of the ZnT3 gene. Proc Natl Acad Sci USA 96:1716–1721

Danielsson J, Pierattelli R, Banci L, Graslund A (2007) High-resolution NMR studies of the zinc-binding site of the Alzheimer's amyloid β-peptide. FEBS J 274:46–59

Deane R, Sagare A, Hamm K et al (2008) apoE isoform-specific disruption of amyloid β peptide clearance from mouse brain. J Clin Invest 118:4002–4013

Deshpande A, Kawai H, Metherate R, Glabe CG, Busciglio J (2009) A role for synaptic zinc in activity-dependent Aβ oligomer formation and accumulation at excitatory synapses. J Neurosci 29:4004–4015

Frederickson CJ, Koh JY, Bush AI (2005) The neurobiology of zinc in health and disease. Nat Rev Neurosci 6:449–462

Friedlich AL, Lee JY, van Groen T et al (2004) Neuronal zinc exchange with the blood vessel wall promotes cerebral amyloid angiopathy in an animal model of Alzheimer's disease. J Neurosci 24:2459–3453

Fryer JD, Taylor JW, DeMattos RB et al (2003) Apolipoprotein E markedly facilitates age-dependent cerebral amyloid angiopathy and spontaneous hemorrhage in amyloid precursor protein transgenic mice. J Neurosci 23:7889–7896

González C, Martín T, Cacho J et al (1999) Serum zinc, copper, insulin and lipids in Alzheimer's disease ε4 apolipoprotein E allele carriers. Eur J Clin Invest 29:637–642

Holtzman DM, Fagan AM, Mackey B et al (2000) Apolipoprotein E facilitates neuritic and cerebrovascular plaque formation in an Alzheimer's disease model. Ann Neurol 47:739–747

Jiang Q, Lee CY, Mandrekar S et al (2008) ApoE promotes the proteolytic degradation of Aβ. Neuron 58:681–693

Kantheti P, Qiao X, Diaz ME et al (1998) Mutation in AP-3 delta in the mocha mouse links endosomal transport to storage deficiency in platelets, melanosomes, and synaptic vesicles. Neuron 21:111–122

Koistinaho M, Lin S, Wu X et al (2004) Apolipoprotein E promotes astrocyte colocalization and degradation of deposited amyloid-β peptides. Nat Med 10:719–726

Kontush A (2005) Amyloid-β: acute-phase apolipoprotein with metal-binding activity. J Alzheimers Dis 8:129–137

Kozin SA, Zirah S, Rebuffat S, Hoa GH, Debey P (2001) Zinc binding to Alzheimer's Aβ (1–16) peptide results in stable soluble complex. Biochem Biophys Res Commun 285: 959–964

Lee JY, Mook-Jung I, Koh JY (1999) Histochemically reactive zinc in plaques of the Swedish mutant β-amyloid precursor protein transgenic mice. J Neurosci 19:RC10

Lee JY, Cole TB, Palmiter RD, Suh SW, Koh JY (2002) Contribution by synaptic zinc to the gender-disparate plaque formation in human Swedish mutant APP transgenic mice. Proc Natl Acad Sci USA 99:7705–7710

Lee JY, Friedman JE, Angel I, Kozak A, Koh JY (2004a) The lipophilic metal chelator DP-109 reduces amyloid pathology in brains of human β-amyloid precursor protein transgenic mice. Neurobiol Aging 25:1315–1321

Lee JY, Kim JH, Hong SH et al (2004b) Estrogen decreases zinc transporter 3 expression and synaptic vesicle zinc levels in mouse brain. J Biol Chem 279:8602–8607

Lovell MA, Robertson JD, Teesdale WJ, Campbell JL, Markesbery WR (1998) Copper, iron and zinc in Alzheimer's disease senile plaques. J Neurol Sci 158:47–52

Masliah E, Mallory M, Ge N, Alford M, Veinbergs I, Roses AD (1995) Neurodegeneration in the central nervous system of apoE-deficient mice. Exp Neurol 136:107–122

Mekmouche Y, Coppel Y, Hochgrafe K et al (2005) Characterization of the ZnII binding to the peptide amyloid-beta1-–16 linked to Alzheimer's disease. Chembiochem 6:1663–1671

Miller LM, Wang Q, Telivala TP, Smith RJ, Lanzirotti A, Miklossy J (2006) Synchrotron-based infrared and X-ray imaging shows focalized accumulation of Cu and Zn co-localized with β-amyloid deposits in Alzheimer's disease. J Struct Biol 155:30–33

Miura T, Suzuki K, Kohata N, Takeuchi H (2000) Metal binding modes of Alzheimer's amyloid β-peptide in insoluble aggregates and soluble complexes. Biochemistry 39:7024–7031

Miyata M, Smith JD (1996) Apolipoprotein E allele-specific antioxidant activity and effects on cytotoxicity by oxidative insults and β-amyloid peptides. Nat Genet 14:55–61

Moir RD, Atwood CS, Romano DM et al (1999) Differential effects of apolipoprotein E isoforms on metal-induced aggregation of Aβ using physiological concentrations. Biochemistry 38:4595–4603

Nakai M, Kawamata T, Taniguchi T, Maeda K, Tanaka C (1996) Expression of apolipoprotein E mRNA in rat microglia. Neurosci Lett 211:41–44

Namba Y, Tomonaga M, Kawasaki H, Otomo E, Ikeda K (1991) Apolipoprotein E immunoreactivity in cerebral amyloid deposits and neurofibrillary tangles in Alzheimer's disease and kuru plaque amyloid in Creutzfeldt-Jakob disease. Brain Res 541:163–166

Näslund J, Thyberg J, Tjernberg LO et al (1995) Characterization of stable complexes involving apolipoprotein E and the amyloid β peptide in Alzheimer's disease brain. Neuron 15:219–228

Offe K, Dodson SE, Shoemaker JT et al (2006) The lipoprotein receptor LR11 regulates amyloid β production and amyloid precursor protein traffic in endosomal compartments. J Neurosci 26:1596–1603

Palmiter RD, Huang L (2004) Efflux and compartmentalization of zinc by members of the SLC30 family of solute carriers. Pflugers Arch 447:744–751

Palmiter RD, Cole TB, Quaife CJ, Findley SD (1996) ZnT-3, a putative transporter of zinc into synaptic vesicles. Proc Natl Acad Sci USA 93:14934–14939

Salazar G, Love R, Werner E et al (2004) The zinc transporter ZnT3 interacts with AP-3 and it is preferentially targeted to a distinct synaptic vesicle subpopulation. Mol Biol Cell 15:575–587

Sanan DA, Weisgraber KH, Russel SJ et al (1994) Apolipoprotein E associates with β amyloid peptide of Alzheimer's disease to form novel monofibrils. J Clin Invest 94:860–869

Saunders AM, Strittmatter WJ, Schmechel D et al (1993) Association of apolipoprotein E allele epsilon 4 with late-onset familial and sporadic Alzheimer's disease. Neurology 43:1467–1472

Stoltenberg M, Bush AI, Bach G et al (2007) Amyloid plaques arise from zinc-enriched cortical layers in APP/PS1 transgenic mice and are paradoxically enlarged with dietary zinc deficiency. Neuroscience 150:357–369

Strittmatter WJ, Saunders AM, Schmechel D et al (1993) Apolipoprotein E: high avidity binding to β-amyloid and increased frequency of type 4 allele in late-onset familial Alzheimer's disease. Proc Natl Acad Sci USA 90: 1977–1981

Suh SW, Jensen KB, Jensen MS et al (2000) Histochemically-reactive zinc in amyloid plaques, angiopathy, and degenerating neurons of Alzheimer's diseased brains. Brain Res 852:274–278

Syme CD, Viles JH (2006) Solution 1H NMR investigation of Zn^{2+} and Cd^{2+} binding to amyloid-beta peptide (Aβ) of Alzheimer's disease. Biochim Biophys Acta 1764: 246–256

Wisniewski T, Frangione B (1992) Apolipoprotein E: a pathological chaperone protein in patients with cerebral and systemic amyloid. Neurosci Lett 135:235–238

Yang DS, McLaurin J, Qin K, Westaway D, Fraser PE (2000) Examining the zinc binding site of the amyloid-β peptide. Eur J Biochem 267:6692–6698

Zhao L, Lin S, Bales KR et al (1993) Macrophage-mediated degradation of β-amyloid via an apolipoprotein E isoform-dependent mechanism. J Neurosci 29:3603–3612

Zirah S, Kozin SA, Mazur AK et al (2006) Structural changes of region 1–16 of the Alzheimer disease amyloid β-peptide upon zinc binding and in vitro aging. J Biol Chem 281: 2151–2161